Research Article

On the methyl and carbon monoxide coupling reaction: A simulation study of acetyl coenzyme-A synthase

Khaleel A. Abu-Sbeih and Tareq Irshaidat*

Department of Chemistry, College of Sciences, Al-Hussein Bin Talal University, Ma'an, Jordan

_____

ABSTRACT

Organic chemistry transformations mediated by transition metals is one of the active and hot inter-disciplinary research topics. ACS/CODH is an important enzyme that catalyzes the formation of acetyl CoA from CO_2 and CH_3. The mechanism by which ACS catalyzes the formation of CH_3CO-$SCoA$ from CO and CH_3 is studied theoretically using DFT and a new nickel model in which the metal is coordinated by three sulfur atoms. The analysis illustrates that the reaction course starts with CO binding to Ni(I) followed by CH_3 binding to form a Ni(II) trigonal bipyramidal intermediate. Ultimately, migration results in the formation of an acetyl intermediate. This path is supported by structural parameters comparable to literature values. The details are new addition to nickel(I) chemistry and allow designing new coordination environment and catalyst models for fine-tuning characteristics of the transformation process.

Key words: acetyl coenzyme synthase, nickel(I), sulfur ligands, DFT, B3LYP.
_____

INTRODUCTION

The acetyl coenzyme A synthase/carbon monoxide dehydrogenase, ACS-CODH, bifunctional enzyme complex is found in several bacteria and has two activities, the ACS activity which catalyzes the synthesis of the all-important acetyl-CoA group from simple starting materials, i.e. CO and CH_3, and the CODH activity which converts CO_2 into CO [1]. CO produced from CODH is consumed by ACS. A good deal of information about the structure of the enzyme was predicted before its X-ray structural determination in 2002 [2]. The $\alpha_2\beta_2$ tetramer has four types of clusters: B, D, C (responsible for CODH activity), and A-clusters. There is one A-cluster per α-subunit, and it is responsible for the ACS activity. The A-cluster is unique in that it contains a 4Fe-4S cubane in addition to the so called proximal nickel, Ni_p, and distal nickel, Ni_d, centers, Figure 1. The presence of two Ni atoms at the active center was confirmed in 2003 [3]. Since then, the efforts of many groups intensified to understand the enzyme better [4-7]. The mechanism is still subject to debate, although there are some important pieces of evidence that help to understand the mechanism. Besides its biochemical importance, the elucidation of the enzymatic mechanism is also essential because of the great environmental impact of CO_2 and the industrial applications of successful models in the synthesis of acetic acid and its derivatives.

Density functional theory is widely used to study both the structures of the compounds and the mechanisms of chemical reactions. The application of DFT to complete enzyme structures or even complex active sites such as that of ACS is a daunting task. Choosing small structural units is a valid way to obtain important information.

In the current work, we chose mononuclear nickel complexes in an all-sulfur environment as model for the Ni_p center of the active site of ACS (Figure 2). This simplification is not far-fetched since there is near consensus that the entire reaction takes place at the so called proximal nickel, which changes oxidation states and geometry during the course of the reaction.
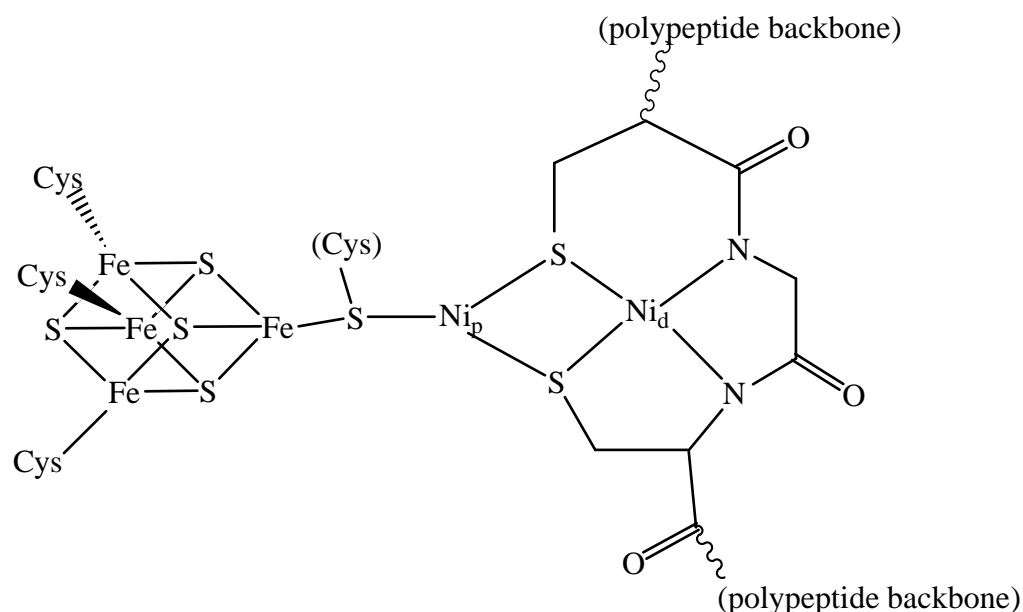
Figure 1: The active site of ACS. Nip may be in equilibrium interaction with a donor atom from the medium
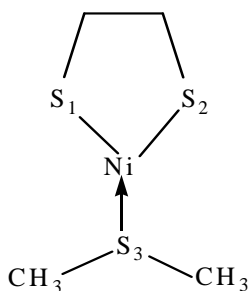
Figure 2: The simulation model that is used in the calculations

EXPERIMENTAL SECTION

The Gaussian 03 suit of programs [8] was used for performing all the calculations. The B3LYP hybrid functional [9] and the Lanl2dz basis set [10-13] were used for geometry optimization and frequency calculations. All the frequencies of the studied structures are positive values which indicate that each is a true minimum on the potential energy diagram. Using the same functional and the optimized geometries the energy was calculated using the 6-31+G(d,p) basis set [14], too. The literature shows that the adopted level of theory can produce acceptable results [15-23].

RESULTS AND DISCUSSION

Acetyl co-enzyme synthase: analyzing the proposed mechanisms in the literature
The distal nickel site in ACS has a Ni(II) atom coordinated by two S atoms from bridging cysteinates and two N atoms from the polypeptide backbone in a near square planar geometry [2]. There is consensus that this "saturated" nickel does not participate in catalysis [1]. The 4Fe-4S center is also not expected to have any roles other than possibly electron transfer to the proximal Ni, the site thought to be the center of ACS catalytic activity. Ni$_p$ has variable oxidation states and geometries during catalytic turnovers.

Before crystal structure determination, two main mechanisms were proposed for the acetyl co-enzyme A synthase activity. In the paramagnetic mechanism, Ragsdale et al. [24] proposed that CO first binds to Ni(I) followed by CH_3^+ donated by methylated corrinoid FeS protein, which generates Ni(III) with both CO and CH_3 bound *cis* to each other. An electron transferred from the FeS cluster generates an octahedral Ni(II) soon after, a step that is followed by methyl migration resulting in a 5-coordinate acetyl Ni(II) species. In the diamagnetic mechanism [25] Barondeau and Lindahl started with a 5-coordinate Ni(II) complex having an extra ligand. Oxidation was suggested to occur on the thiolates rather than the nickel, which remains in the +2 oxidation state.

_____

Following determination of the structure, two new mechanisms were proposed. Fontecilla-Camps et al. [3] proposed formation of a tetrahedral Ni(0) center upon binding CO to the proximal Ni. A square pyramidal Ni(II) center then results from the addition of CH_3^+ with both CO and CH_3 *cis* to each other. Migration produces an acetyl Ni(II) intermediate. Attack by CoAS⁻ produces acetyl CoA. The second mechanism proposed by Hall et al. [4] again uses Ni(0) and ends with Ni(II). However, according to this mechanism, a square planar intermediate is formed upon the addition of CO and CH_3, after the dissociation of one of the enzyme's ligating sulfur atoms.

What do we know about ACS?
In order to propose an acceptable mechanism, the following experimental facts have to be taken into consideration:

1- The A-cluster of ACS has been shown to exist in two oxidation states, the diamagnetic oxidized state and the paramagnetic reduced state [5, 26]

2- When the oxidized state is reduced under CO atmosphere, a paramagnetic reduced state- CO intermediate is formed which exhibits a characteristic EPR signal [27, 28] .This intermediate is also characterized by a strong stretching frequency at 1996 cm⁻¹ in the IR spectrum, indicative of a terminal CO ligand with significant back-donation [29, 30].

3- Mössbauer spectra of the active site indicate an exchange-coupled S = 0 $\{[Fe_4S_4]^{1+} Ni_p^{1+}\}$ state.[5] Additional treatment with CO caused a change in the Mössbauer parameters, suggesting that there is an interaction with a bound CO, but without altering the $\{[Fe_4S_4]^{1+} Ni_p^{1+}\}$ state. Reduction of this state afforded an EPR signal typical of Ni^{1+} ions.

4- During enzymatic turnover, an EPR-silent intermediate [6] is formed as a result of the transfer of a methyl group from the cobalt-methyl moiety of methylated-corrinoid-iron-sulfur protein to the A-cluster [31].

5- There are no known methyl transfer reactions from a Co-CH_3 complex to a Ni(0) complex, but there is precedence in the literature for methyl transfer from Co-CH_3 to Ni(I) resulting in the formation of $CH_3Ni(II)$ [32, 33].

6- The presence of Ni(0) in enzymatic systems is unknown and there is no consensus that it exists in ACS either [6, 34].

A Theoretical model of ACS mechanism
In the current work, we used a simple model of low coordinate mononuclear nickel with an all sulfur environment similar to the one surrounding Ni_p in ACS, Figure 2. The oxidation states 0 (singlet), +1 (doublet), +2 (both singlet and triplet), and +3 (both doublet and quartet) were all used in search of energy minima along the course of consecutive substrate binding and migration. Structure optimization and energy minimization were performed using density functional theory- B3LYP functional with LanL2DZ being used as the basis set. Optimization was first done with two thiolates bonded to Ni then one and two hydrogen atoms were added, respectively, for comparison with the complexes that have no protons present on the thiolates. Energies are shown in Tables 1-3. Energy was also calculated using 6-31+G(d,p) as the basis set, Tables 4-6. Plots showing the dependence of energy (6-31+G(d,p) data) on various oxidations states, spin states, and geometries are shown in Figures 3 and 4.

Table 1. The energy values (Hartree) for the nickel complexes with no hydrogen atoms added using B3LYP functional and LanL2DZ basis set

Structure	Ni(0)	Ni(I)	Ni(II) HS	Ni(II) LS	Ni(III) HS	Ni(III) LS
NiS_3	a	-358.152281	-358.089866	-358.077754	-357.820193	-357.815710
NiS_3CO	a	-471.481198	-471.396083	-471.410177	-471.132976	-471.123817
NiS_3Me	a	a	a	-398.045880	-397.949439	-397.970593
NiS_3MeCO	a	a	a	-511.343200	-511.243933	-511.268381
NiS_3COMe	a	a	-511.374380	-511.378757	-511.274712	-511.294550

a: structure was distorted, HS: high spin, LS: low spin.

Table 2. The energy values (Hartree) for the nickel complexes with one hydrogen atom added using B3LYP functional and LanL2DZ basis set

Structure	Ni(0)	Ni(I)	Ni(II) HS	Ni(II) LS	Ni(III) HS	Ni(III) LS
NiS_3	-358.665889	-358.675998	-358.440614	-358.423358	-357.991768	-357.979878
NiS_3CO	a	-471.994663	-471.750929	-471.756097	-471.313683	-471.318016
NiS_3Me	a	a	-398.556669	-398.561470	-398.302667	-398.320075
NiS_3MeCO	a	a	-511.854946	a	-511.592757	-511.623978
NiS_3COMe	a	a	-511.877143	-511.886603	-511.624553	-511.649160

a: structure was distorted, HS: high spin, LS: low spin.

Table 3. The energy values (Hartree) for the nickel complexes with two hydrogen atoms added using B3LYP functional and LanL2DZ basis set

Structure	Ni(0)	Ni(I)	Ni(II) HS	Ni(II) LS	Ni(III) HS	Ni(III) LS
NiS$_3$	-359.201277	-359.047684	-358.621605	-358.603618	a	a
NiS$_3$CO	-472.553190	-472.363135	-471.941775	-471.948797	a	a
NiS$_3$Me	a	a	-398.919981	-398.926613	-398.495806	-398.516513
NiS$_3$MeCO	a	a	-512.218804	-512.236666	-511.796934	-511.828298
NiS$_3$COMe	a	a	-512.241773	-512.249657	-511.831458	-511.859584

a: structure was distorted, HS: high spin, LS: low spin.

Table 4. The energy values (Hartree) for the nickel complexes with no hydrogen atoms added using B3LYP functional and 6-31+G(d,p) basis set

Structure	Ni(0)	Ni(I)	Ni(II) HS	Ni(II) LS	Ni(III) HS	Ni(III) LS
NiS$_3$	a	-2861.342830	-2861.279406	-2861.270428	-2861.013830	-2861.014201
NiS$_3$CO	a	-2974.697762	-2974.615132	-2974.633331	-2974.355007	-2974.346137
NiS$_3$Me	a	a	A	-2901.251886	-2901.149612	-2901.174035
NiS$_3$MeCO	a	a	A	-3014.574193	-3014.464894	-3014.500568
NiS$_3$COMe	a	a	-3014.592722	-3014.605310	-3014.495875	-3014.520299

a: structure was distorted, HS: high spin, LS: low spin.

Table 5. The energy values (Hartree) for the nickel complexes with one hydrogen atom added using B3LYP functional and 6-31+G(d,p)) basis set

Structure	Ni(0)	Ni(I)	Ni(II) HS	Ni(II) LS	Ni(III) HS	Ni(III) LS
NiS$_3$	-2861.888919	-2861.875582	-2861.643886	-2861.631806	-2861.196053	-2861.193488
NiS$_3$CO	a	-2975.223051	-2974.983291	-2974.994755	-2974.548251	-2974.560208
NiS$_3$Me	a	a	-2901.764744	-2901.777667	-2901.516238	-2901.539008
NiS$_3$MeCO	a	a	-3015.091747	a	-3014.826305	-3014.864091
NiS$_3$COMe	a	a	-3015.106440	-3015.124884	-3014.855069	-3014.887162

a: structure was distorted, HS: high spin, LS: low spin.

Table 6. The energy values (Hartree) for the nickel complexes with two hydrogen atoms added using B3LYP functional and 6-31+G(d,p) basis set

Structure	Ni(0)	Ni(I)	Ni(II) HS	Ni(II) LS	Ni(III) HS	Ni(III) LS
NiS$_3$	-2862.430799	-2862.258212	-2861.837636	-2861.826655	a	a
NiS$_3$CO	-2975.796869	-2975.601954	-2975.189188	-2975.202914	a	a
NiS$_3$Me	a	a	-2902.138337	-2902.153433	-2901.721716	-2901.743047
NiS$_3$MeCO	a	a	-3015.466374	-3015.488838	-3015.048255	-3015.084347
NiS$_3$COMe	a	A	-3015.482081	-3015.498765	-3015.079895	-3015.109918

a: structure was distorted, HS: high spin, LS: low spin.
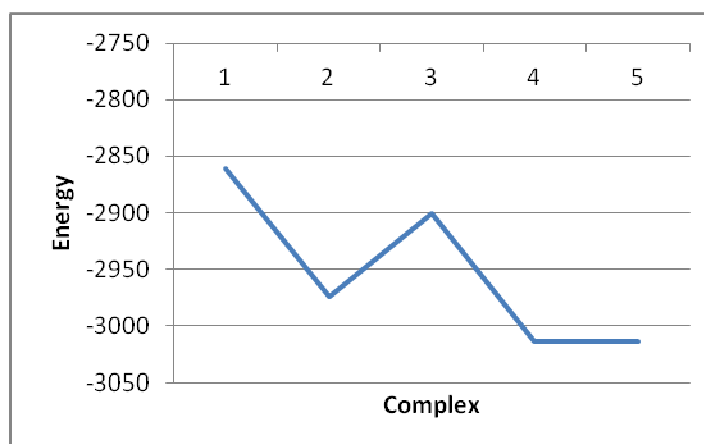
Figure 3. Energy change (atomic units) as more reactants are added to nickel using 6-31G+(d,p) (no hydrogen atoms are added to the complex) (1 (NiS$_3$), 2 (NiS$_3$CO), 3 (NiS$_3$Me), 4 (NiS$_3$MeCO), 5 (NiS$_3$COMe))

Inspection of the data presented in the tables and Figures 3 and 4 shows the following. The preferred order of binding was always found to be CO then CH$_3$, which binds *cis* to CO. From plots of energy versus oxidation state and spin state, the course of reaction with minimum energy is that for CO binding to Ni(I) followed by methyl binding which causes oxidation of nickel to Ni(II), in a low-spin state (LS). Nickel remains in the +2 oxidation state as the acetyl intermediate is formed afterwards.

_____

The Ni(0) models were generally subjected to severe distortion whereby ligands were either split away from Ni or parts of them split off probably because of too much charge being accumulated at the thiolate-coordinated nickel(0) center. Ni(I) was always distorted when bonded to a methyl or acetyl ligand, indicating that it is unstable in a thiolate rich environment unless some back-bonding ligands such as CO are present in its coordination sphere. Ni(III) was not energetically preferred in any case, neither as a doublet (LS) nor as a quartet (HS). No hydrogen atoms are expected to be bound to the sulfur atoms coordinated to nickel as the reaction progresses and the oxidation state of nickel increases. The presence of protons destabilizes the system in higher Ni oxidation states.

(a)   NiS₃

(b) NiS₃CO   **(c) NiS₃Me**

(d) NiS₃MeCO   **(e) NiS₃COMe**
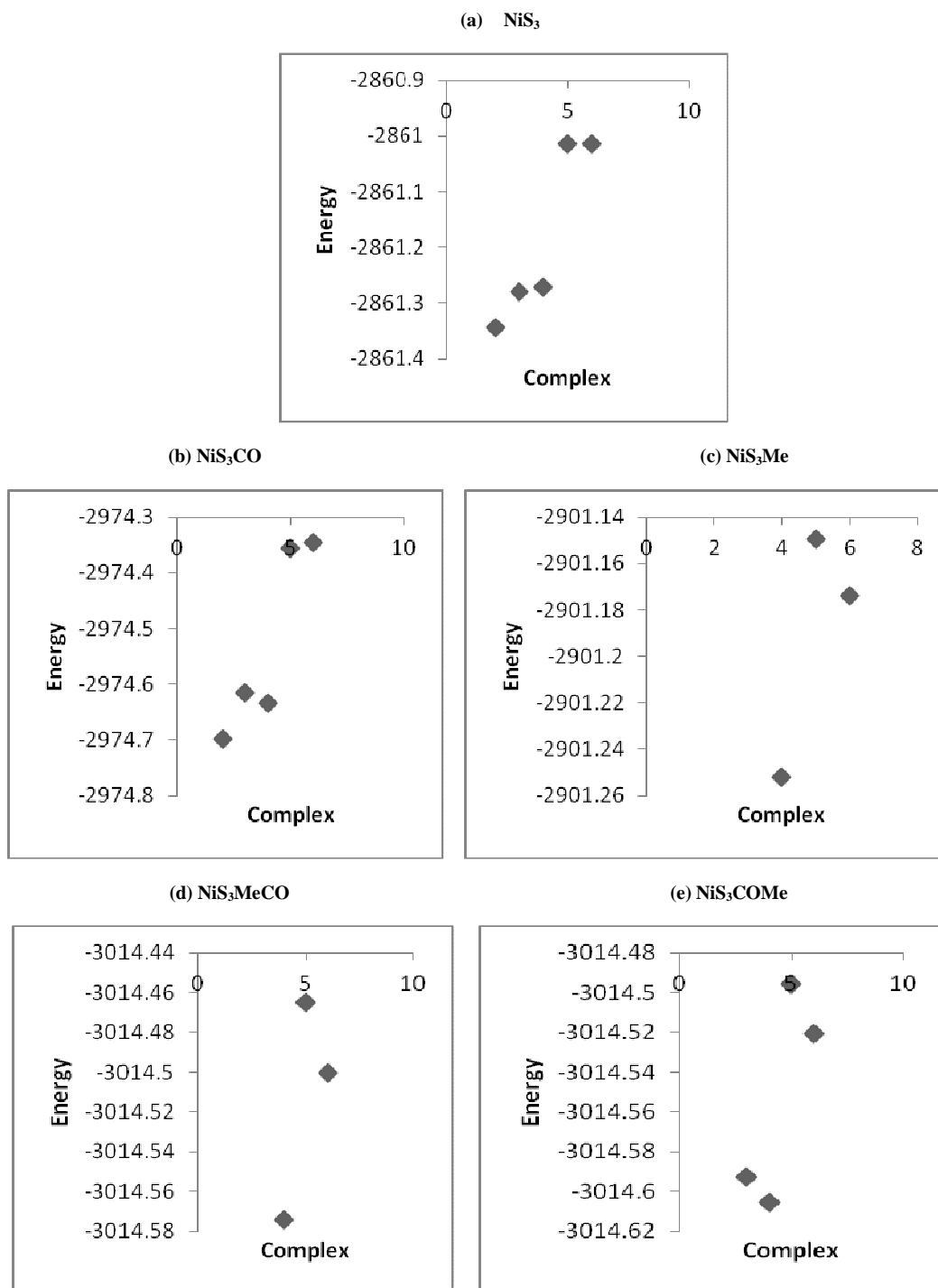
Figure 4. Energy change (atomic units) as a function of the oxidation state and spin state for the five complex structures using 6-31G+(d,p)
(no hydrogen added) (1 (Ni(0)), 2 (Ni(I)), 3 (Ni(II) HS), 4 (Ni(II) LS), 5 (Ni(III) HS), 6 (Ni(III) LS); HS: high spin, LS: low spin).

The following mechanism, Scheme I, which we propose here, takes into account all of the previously mentioned experimental facts (section 3.2) as well as the results of our theoretical investigations. Ni_p is first reduced from the diamagnetic square planar Ni(II) to a paramagnetic Ni(I) state. This reduced state then binds CO with no change in the oxidation state of Ni. A methyl moiety is then transferred from methylated-corrinoid-iron-sulfur protein to form a trigonal bipyramidal intermediate with concomitant oxidation of nickel to Ni(II). The resulting intermediate, diamagnetic, has both CO and CH_3 *cis* to each other. Migration of CH_3 to the neighboring CO forms a Ni(II)-$COCH_3$ intermediate. Finally, the acetyl group in Ni(II)-$COCH_3$ is transferred to the thiolate group of co-enzyme A thus producing acetyl CoA and restoring the reduced A-cluster, ready to start another catalytic cycle.
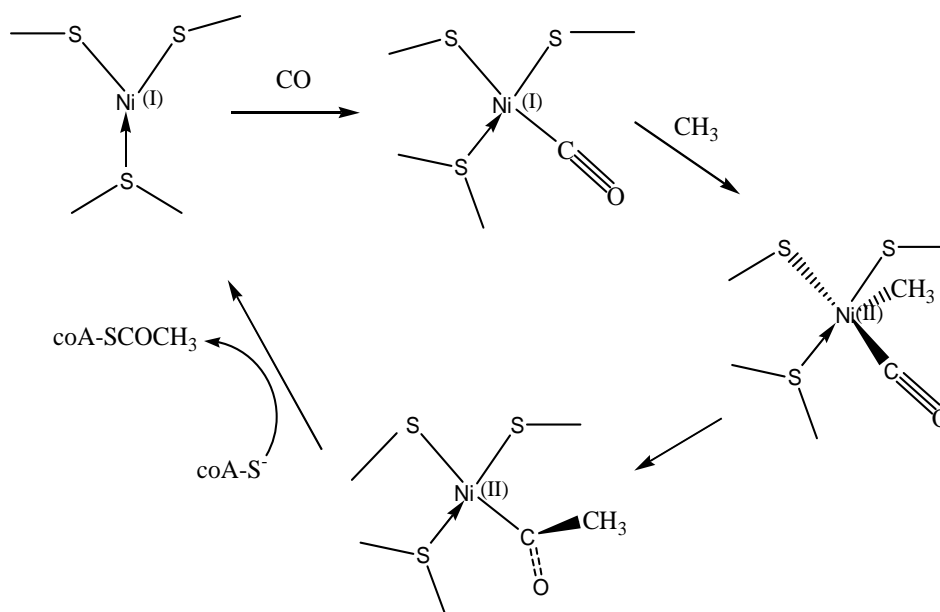
Scheme I. Proposed mechanism of ACS

This suggested mechanism complies with the experimental data obtained for the enzyme. The paramagnetic intermediate in the reduced ACS is expected to be Ni(I) and the diamagnetic intermediate Ni(II) [5, 7]. Ni(0) is not present in biological environments [34] and is not very likely to be present in an all-sulfur electron-rich environment in the reduced state of ACS. On the other hand, Ni(III) is highly oxidizing and is not expected to be stable in the presence of the soft polarizable cystinate ligands. Moreover, Ni(III) is rare in chemical models [35] as well as in biological systems were it is thought to be present in the oxidized states of the enzyme FeNi hydrogenase [36] and the enzyme Ni-SOD [37].

Structural data of Scheme I compounds
Structural data for the model complexes that appear in the mechanism are presented in Tables 7 and 8. The NiS_3 complex has a near T-shaped structure which turns into the square planar NiS_3CO upon binding CO, Figure 5. Methyl binding transforms the compound into the trigonal bipyramidal geometry, which upon methyl migration, returns back into the square planar geometry forming the acetyl complex in the process.

Ni-S bond lengths were in the range known for nickel complexes [38-40]. A notable exception is observed in the NiS_3CO complex where the Ni(I)-ether sulfur bond appears to be too long (2.7622 Å). This distance is longer than the 2.6446 Å Ni(II)-S distance reported by M. L. Calatayud et al. for dithiosquarate complexes of nickel(II) containing 1,10-phenanthroline as a co-ligand [40]. Other than this anomaly, Ni-S bonds were longest in the 5-coordinate NiS_3MeCO complex.

Ni-CH_3 bond distances are very close to the 1.966 Å Ni(II)-CH_3 bond distance reported by Dougherty, W. G. for square planar nickel(II) [41]. Ni(II)-COMe bond distance is about 0.06 Å shorter than the Ni-CH_3 bond as observed by Holm and co-workers [41, 43]. The CO bond distance in these latter complexes is in the range of 1.27 Å indicative of double bond character. Finally, the bond distances of the terminally coordinated CO, both in NiS_3CO and NiS_3MeCO, are longer than expected for terminally bound CO indicative of extensive back-donation in the electron-rich thiolate complexes [44]. This lengthening of the CO bond draws similarities to the strong back-donation observed in ACS during its catalytic turnover [39, 40].

_____

(a)

(b)

(c)

(d)

(e)
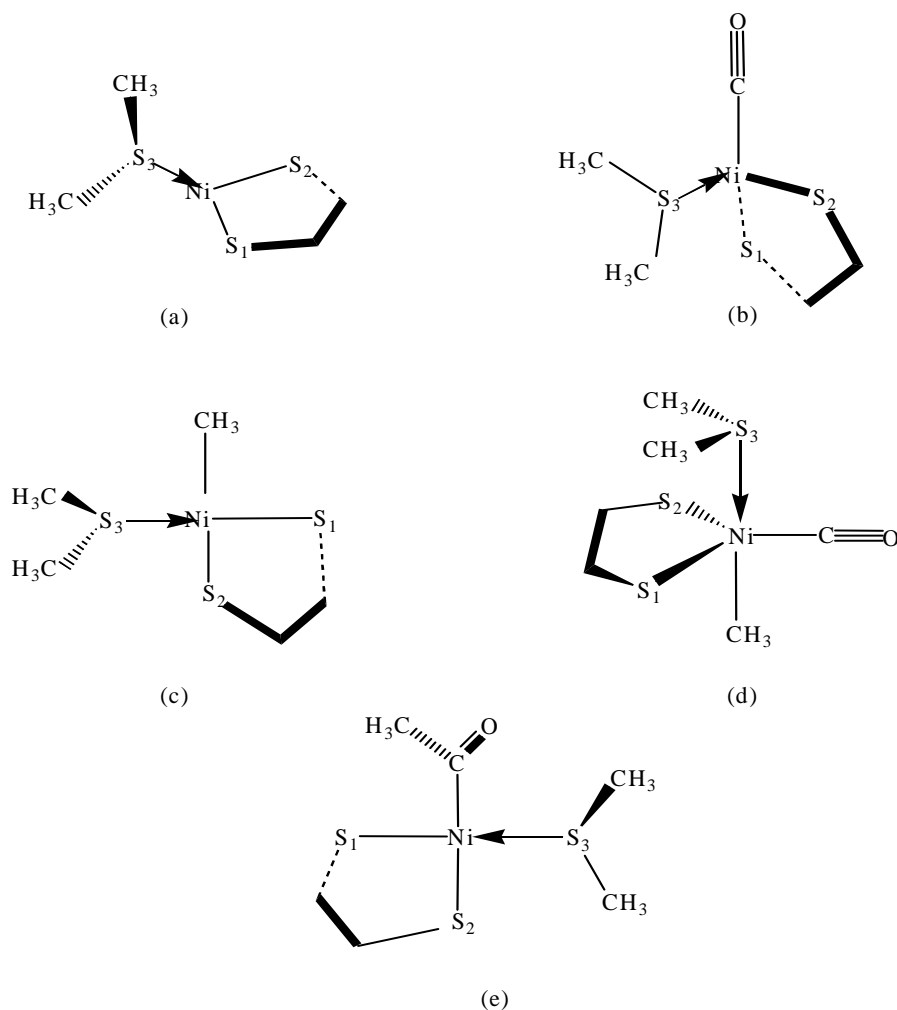
Figure 5. Optimized structures of the compounds presented in Scheme I

Table 7. Bond distances of Scheme I compounds

Bond	Bond length (Å)				
	NiS$_3$	NiS$_3$CO	NiS$_3$Me	NiS$_3$MeCO	NiS$_3$COMe
NiS1	2.38905	2.37669	2.25866	2.40560	2.27729
NiS2	2.30191	2.342438	2.37613	2.41412	2.36979
NiS3	2.40112	2.7622	2.39435	2.59653	2.39747
Ni(CH$_3$)	-	-	1.96761	1.97298	-
NiC(O)	-	1.80799	-	1.78349	-
NiC((O)CH$_3$)	-	-	-	-	1.91734
CO	-	1.18938	-	1.19229	1.26880

Table 8. Bond angles of Scheme I compounds

Angle	Bond angle (Degrees)				
	NiS$_3$	NiS$_3$CO	NiS$_3$Me	NiS$_3$MeCO	NiS$_3$COMe
S1NiS2	99.637	95.233	92.294	93.599	90.765
S1NiS3	100.029	93.211	176.383	92.473	178.723
S2NiS3	160.19	131.661	90.625	94.252	90.307
S1Ni(CH$_3$)	-	-	89.233	90.568	-
S2Ni(CH$_3$)	-	-	178.426	92.363	-
S3Ni(CH$_3$)	-	-	87.863	172.531	-
S1Ni(CO)	-	142.495	-	137.878	-
S2Ni(CO)	-	103.926	-	128.484	-
S3Ni(CO)	-	97.403	-	86.742	-
S1Ni(COCH$_3$)	-	-	-	-	89.238
S2Ni(COCH$_3$)	-	-	-	-	179.973
S3Ni(COCH$_3$)	-	-	-	-	89.690
NiCO	-	171.337	-	175.247	123.159
(CH$_3$)Ni(CO)	-	-	-	86.427	-

CONCLUSION

The theoretical study presented in this paper gives evidence for the binding of CO to Ni(I) followed by CH_3 binding. This generates a trigonal bipyramidal intermediate of Ni(II) with both CO and CH_3 *cis* to each other which facilitates the next step in which the methyl migrates to form a square planar acetyl intermediate of Ni(II). The acetyl group is finally transferred to $CoAS^-$. This mechanism complies with the data collected for ACS and presents an acceptable alternative for the previously proposed mechanisms. Successful synthesis of the intermediates proposed in this mechanism will be helpful to prove its credibility.

REFERENCES

[1] DJ Evans, *Coord. Chem. Rev.*, **2005**, 249, 1582-1595.
[2] TI Doukov, TM Iverson, J Seravalli, SW Ragsdale, CL Drennan, *Science*, **2002**, 298, 567-572.
[3] C Darnault, A Volbeda, EJ Kim, P Legrand, X Vernède, PA Lindahl, JC Fontecilla-Camps, *Nat. Struct. Biol.*, **2003**, 10, 271-279.
[4] CE Webster, MY Darensbourg, PA Lindahl, MB Hall, *J. Am. Chem. Soc.*, **2004**, 126, 3410-3411.
[5] X Tan, M Martinho, A Stubna, PA Lindahl, E Münck, *J. Am. Chem. Soc.,* , **2008**, 130, 6712-6713.
[6] PA Lindahl, *J. Biol. Inorg. Chem.*, **2004**, 9, 516-524.
[7] G Bender, TA Stich, L Yan, RD Britt, SP Cramer, SW Ragsdale, *Biochemistry*, **2010**, 49, 7516–7523.
[8] Gaussian 03, Revision E.1, MJ Frisch, GW Trucks, HB Schlegel, GE Scuseria, MA Robb, JR Cheeseman, JA Montgomery, JrT Vreven, KN Kudin, JC Burant, JM Millam, SS Iyengar, J Tomasi, V Barone, B Mennucci, M Cossi, G Scalmani, N Rega, GA Petersson, H Nakatsuji, M Hada, M Ehara, K Toyota, R Fukuda, J Hasegawa, . Ishida, T Nakajima, Y Honda, O Kitao, H Nakai, M Klene, X Li, JE Knox, HP Hratchian, JB Cross, C Adamo, J Jaramillo, R Gomperts, RE Stratmann, O Yazyev, AJ Austin, R Cammi, C Pomelli, JW Ochterski, PY Ayala, K Morokuma, GA Voth, P Salvador, JJ Dannenberg, VG Zakrzewski, S Dapprich, AD Daniels, MC Strain, O Farkas, DK Malick, AD Rabuck, K Raghavachari, JB Foresman, JV Ortiz, Q Cui, AG Baboul, S Clifford, J Cioslowski, BB Stefanov, G Liu, A Liashenko, P Piskorz, I Komaromi, RL Martin, DJ Fox, T Keith, MA Al-Laham, CY Peng, A Nanayakkara, M Challacombe, PMW Gill, B Johnson, W Chen, MW Wong, C Gonzalez, JA Pople, Gaussian, Inc., Pittsburgh PA, 2003.
[9] AD Becke, *J. Chem. Phys.,* 1993, 98, 5648-5653.
[10] TH Dunning Jr., PJ Hay, in *Modern Theoretical Chemistry*, Ed. H. F. Schaefer III, Vol. 3, Plenum, New York, **1976**; 1-28.
[11] PJ Hay, WR Wadt, *J. Chem. Phys.* , **1985**, 82, 270-277.
[12] WR Wadt, PJ Hay, *J. Chem. Phys.*, **1985**, 82, 284-291.
[13] PJ Hay, WR Wadt, *J. Chem. Phys.*, **1985**, 82, 299-305.
[14] VA Rassolov, MA Ratner, JA Pople, PC Redfern, LA Curtiss, *J. Comp. Chem.*, **2001**, 22, 976.
[15] NL Bill, M Ishida, S Bähring, JM Lim, S Lee, CM Davis, VM Lynch, KA Nielsen, JO Jeppesen, K Ohkubo, S Fukuzumi, D Kim, JL Sessler, *J. Am. Chem. Soc.*, **2013**, *135* (29), 10852–10862.
[16] N Taxak, B. Patel, PV Bharatam, *Inorg. Chem.*, **2013**, *52* (9), 5097–5109.
[17] RK Gupta, R Pandey, R Singh, N Srivastava, B Maiti, S Saha, P Li, Q Xu, DS. Pandey, *Inorg. Chem.*, **2012**, *51* (16), 8916–8930.
[18] SR Daly, JM Keith, ER Batista, KS Boland, SA Kozimor, RL Martin, BL Scott, *Inorg. Chem.*, **2012**, *51* (14), 7551–7560.
[19] D Majumdar, S Roszak, J Leszczynski, *J. Phys. Chem. A*, **2010**, *114* (12), 4340–4353.
[20] SO Nilsson Lill, PEM Siegbahn, *Biochemistry*, **2009**, *48* (5), 1056–1066.
[21] P Bharati, A Bharti, MK Bharty, B Maiti, RJ Butcher, NK Singh, *Polyhedron*, **2013**, 63(31), 156-166.
[22] H Zhang, H Zhao, X Ren, H Duan, Z Tian, Q Meng, *Inorganica Chimica Acta*, **2010**, 363(13), 3530-3537.
[23] R Takjoo, R Centore, M Hakimi, SA Beyramabadi, A Morsali, *Inorganica Chimica Acta*, **2011**, 371(1), 36-41.
[24] J Seravalli, M Kumar, SW Ragsdale, *Biochemistry*, **2002**, 41, 1807-1819.
[25] DP Barondeau, PA Lindahl, *J. Am. Chem. Soc.*, **1997**, 119, 3959-3970.
[26] SW Ragsdale, M Kumar, *Chem. Rev.*, **1996**, 96, 2515-2540.
[27] SW Ragsdale, HG Wood, WE Antholine, *Proc. Natl. Acad. Sci. U.S.A.*, **1985**, 82, 6811-6814.
[28] CM Gorst, SW Ragsdale, *J. Biol. Chem.*, **1991**, 266, 20687-20693.
[29] M Kumar, SW Ragsdale, *J. Am. Chem. Soc.*, **1992**, 114, 8713-8715.
[30] J Chen, S Huang, J Seravalli, JrH Gutzman, DJ Swartz, SW Ragsdale, KA Bagley, *Biochemistry*, **2003**, 42, 14822-14830.
[31] N Ando, Y Kung, M Can, G Bender, SW Ragsdale, CL Drennan, *J. Am. Chem. Soc.*, **2012**, 134, 17945–17954.

_____

[32] MS Ram, CG Riordan, *J. Am. Chem. Soc.*, **1995**, 117, 2365-2366.

[33] SW Ragsdale, CG Riordan, *J. Biol. Inorg. Chem.*, **1996**, 1, 489-493.

[34] TC Harrop, PK Mascharak, *Coord. Chem. Rev.*, **2005**, 249, 3007-3024.

[35] CM Lee, CH Chen, FX Liao, CH Hu, GH Lee, *J. Am. Chem. Soc.*, **2010**, 132, 9256–9258.

[36] H Ogata, W Lubitz, Y Higuchi, *Dalton Trans*, **2009**, 37, 7577–7587.

[37] Y Liu, Q Wang, Y Wei, YW Lin, W Li, JH Su, Z Wang, Y Tian, ZX Huang, X Tan, *Chem. Commun.*, **2013**, 49, 1452-1454.

[38] TW Chiou, WF Liaw, *C. R. Chimie*, **2008**, 11, 818-833.

[39] M Ito, M Kotera, Y Song, T Matsumoto, K Tatsumi, *Inorg. Chem.*, **2009**, 48, 1250-1256.

 [40] ML Calatayud, J Sletten, I Castro, M Julve, G Seitz, K Mann, *Inorg. Chim. Acta*, , **2003**, 353, 159-167.

[41] WG Dougherty, K Rangan, MJ O'Hagan, GPA Yap, CG Riordan, *J. Am. Chem. Soc.*, **2008**, 130, 13510-13511.

[42] GC Tucci, RH Holm, *J. Am. Chem. Soc.*, **1995**, 117, 6489–6496.

[43] P Stavropoulos, MC Muetterties, M Carrie, RH Holm, **1991**, 113, 8485–8492.

[44] RK Hocking, TW Hambley, *Chem. Commun.* **2003**, 1516-1517.